

Improvement Solar Cell based on CIGSSe by a FORS-HET Software

Ammar J. Aswad¹, N. K. Hassan², Adnan R. Ahmed³

^{1,2,3}*Department of physics, Collage of Education for pure science, Tikrit University, Tikrit, Iraq*

E-mail:ammар.j.aswad@st.tu.edu.iq

abstract:

In this study, the FORS-HET software was used for numerical analysis of a solar cell based on Cu (In, Ga) (Se, S) 2 (CIGSSe) absorber layer, with a buffer layer ZnO:B (BZO) and Zn_{0.8}Mg_{0.2}O (ZMO) window layer without CdS. The effect of changing the thickness with changing the doping concentration was taken for both the (CIGSSe) absorption and the buffer layer (BZO), to study the electrical cell properties. The solar energy conversion efficiency is 29.29%, the filling factor is 85.59%, the open circuit voltage is 783.1 mV, the short circuit current is 43.7 mA. Then take the effect of changing layers of buffer on the performance of this cell, and find the (BZO) buffer layer best of In₂S₃, CdS, ZnS, ZnSe respectively.

Keywords: FORS-HET software, CIGSSe, BZO, ZMO.

Introduction:

One of the most promising technologies for manufacturing low-cost, high-efficiency thin film photovoltaics is thin film processing for production Cu (In, Ga) (Se, S) 2 (CIGS) thin film photovoltaics [1]. Due to their different properties, CIGSSe solar cells have been extensively studied. CIGSSe solar cells can attain over 20% performance, which is very effective as compared to high-quality silicon-based crystalline solar cells in small sizes [2]. Solar Frontier K.K. (SF) has set a new world record for efficiency, with a result of 23.35 percent [3].

It is possible to use doping zinc oxide as a suitable layer due to its characteristics, such as the energy gap of 3.3 eV, its toxicity and environmental impact less than CdS, as well as its cost is lower [4]. Therefore, many researcher studies use doping zinc oxide as a buffer layer in CIGS solar cells could attain high conversion efficiencies of 10.29% (Alan Delahoy, et al. 2000) where used (ZnO:Al) [5], 13.9% (Sutichai Chaisitsak, et al. 2001) where used (i-ZnO) with (ZnO:B) window layer [6], 14.5% (M. Bar, et al. 2003) where used (ZnO:Ga) [4], 7.52% (V. Khomyak, et al. 2015) where used (i-ZnO) with (ZnO:Al) window layer [7], 18.4% (Shogo Ishizuka, et al. 2018) where used (ZnO:B) [8].

In this article, a solar cell is modeled and simulated, improved to obtain the best variants of thickness and doping concentration of absorber, buffer layers by AFORS-HET software and take the effect of change different buffer layers.

Simulation parameters for device:

The solar cell structure is: Mo/CIGSSe/ZnO:B(BZO)/ Zn_{0.8}Mg_{0.2}O(ZMO)//MgF₂, and the table.1, table.2 and table.3 has been included all the simulation parameters that is simulated in

FORS-HET software. The properties of Cu ($\text{In}_{(1-x)} \text{Ga}_x$) ($\text{Se}_{(1-y)} \text{S}_y$)₂ (CIGSSe) absorber layer limited by graded between the ratio $x = \text{Ga}/(\text{Ga}+\text{In})$ and $y = \text{S}/(\text{S}+\text{Se})$, to determine this property, we use the equations from references [9,10].

Table 1. Material properties of layers

parameters	Symbol(unit)	MoS ₂ [11]	CIGSSe	ZMO [12]	BZO [13,14]
Thickness	d (cm)	1E-6	5E-5 – 3E-4	5E-6	5E-5
Dielectric constant	dk	13.6	14.89	9	9
Electron Affinity	χ (eV)	4.2	4.25	4.18	4.55
Band gap	E _g (eV)	1.29	1.08	3.69	3.3
Density of states in CB	N _c (cm ⁻³)	2.2E18	2.2E17	1E16	3E18
Density of states in VB	N _v (cm ⁻³)	1.8E19	1.8E19	1E17	1.8E19
Electron mobility	μ_n (cm ² /Vs)	100	103.5	50	100
Hole mobility	μ_p (cm ² /Vs)	150	26.22	20	31
Acceptor concentration	N _a (cm ⁻³)	1E20	1E15 – 1E17	0	0
Donor concentration	N _d (cm ⁻³)	0	0	1E20	1E20
Thermal velocity of electron and hole	v (cm/s)	1E07	1E07	1E07	1E07
density	Rho (g*cm ⁻³)	5.06	5.73	5.2	5.61

Table.2 properties Bulk Gaussian defect states

parameters	Symbol (unit)	CIGSSe	ZMO	BZO
Gaussian defect density	N _t (cm ⁻³)	5.1E14(D)	1E16(A)	1E17(A)
Electron capture cross section	σ_n (cm ²)	1E-16	1E-15	1E-12
Hole capture cross section	σ_p (cm ²)	1E-15	1E-12	1E-15

Table.3 Interface Gaussian defect states

parameters	Symbol (unit)	CIGSSe/BZO
Gaussian defect density	N _t (cm ⁻³)	1E15(D)
Electron capture cross section	σ_n (cm ²)	1E-13
Hole capture cross section	σ_p (cm ²)	1E-15

Result and discussion:

a- effect the thickness and doping concentration on absorber layer:

The first step we will start by changing the thickness of the absorption layer (CIGSSe) from $(1\text{E}-4\text{--}2\text{E}-4)$ cm with changing the doping concentration $(1\text{E}16\text{--}1\text{E}17)$ cm^{-3} , at thickness and doping concentration $(30\text{nm}, 1\text{E}18\text{cm}^{-3})$, $(100\text{nm}, 1\text{E}20\text{cm}^{-3})$ for BZO buffer layer and ZMO widow layer respectively,

we note that with increasing concentration the efficiency of the solar cell increases and also the efficiency increases by the thickness increases to a certain extent and then decreases and is almost fixed at large thickness, the best result is at 1400nm thickness and at a concentration of $1\text{E}17$, and we obtain the output parameters of the solar cell is V_{oc} , J_{sc} , FF , Eff equal $(783.1\text{mV}, 43.7 \text{ mA/cm}^2, 85.59\%, 29.29\%)$ respectively. The figure (1) shows these results.

Here the efficiency increases from the absorption layer for two reasons: The first reason for increasing the efficiency by increasing the doping concentration leads to an increase in the electric field and this improves the collector of the photovoltaic carriers thus increasing the conversion performance. Thus, higher electric field reduces saturation current which basically increases V_{oc} [3], and increase in doping concentration has little effect on J_{sc} within this range.

The second reason for increasing the efficiency by increasing the thickness leads to an increase in the short circuit current due to the increase in the thickness of the absorption layer for a longer wavelength, this means that more photons are absorbed and more pairs of electronic holes are generated [8], and the increase in thickness leads to a slight effect of V_{oc} within this range, This is in agreement with the researchers [9,10] As the short circuit current increases and the open circuit voltage increases, this increases the efficiency of the solar cell.

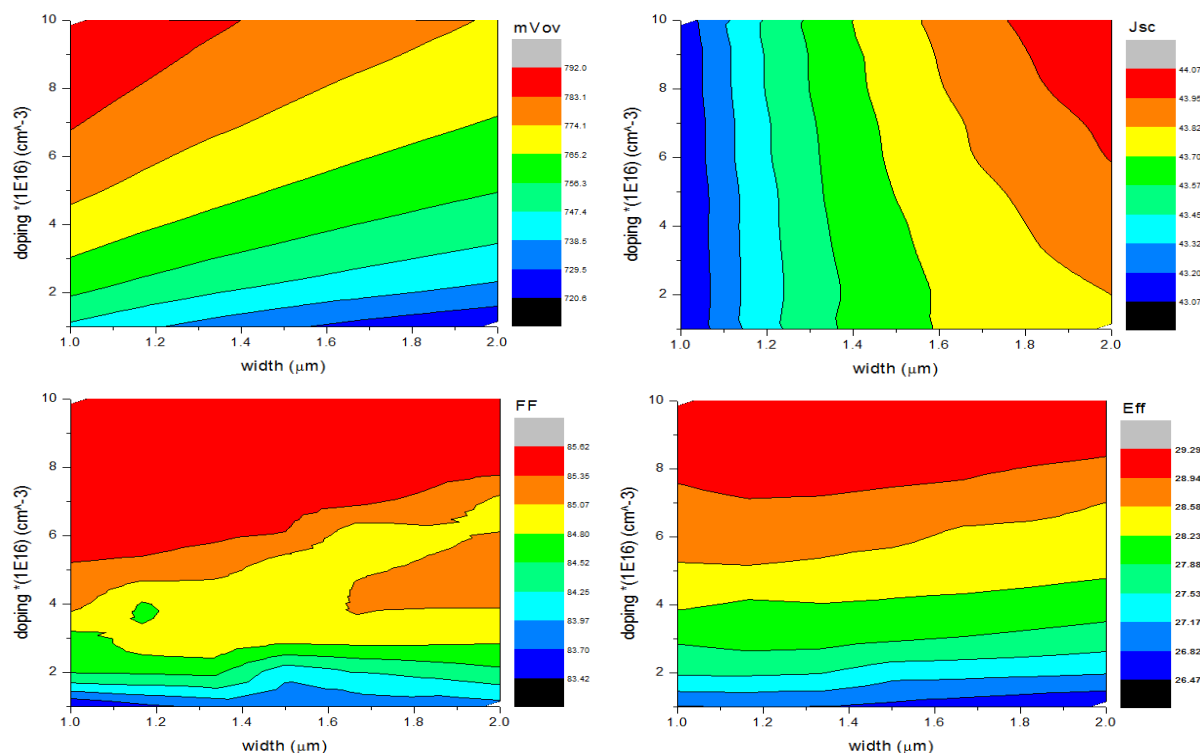


Fig. 1 Photovoltaic parameters as function of changing the thickness with changing the doping concentration of CIGSSe layer

b- effect the thickness and doping concentration on buffer layer:

The second step after the best result in absorber layer, we will be changing the thickness of the buffer layer (BZO) from (1E-6-1E-5) cm with changing the doping concentration (1E18-1E19) cm⁻³, at thickness (100)nm and doping concentration (1E20) cm⁻³ for ZMO widow layer. We note that output parameter cell effected by: first, thickness, the lower the thickness, the greater the efficiency, the open circuit voltage decreases with increasing thickness, the filling factor is slightly increasing with increasing thickness, the short-circuit current decreases with increasing thickness with change doping concentration, because increase the buffer layer thickness lead to more photons are absorbed in it and only a small number of photons reach the CIGS absorbing layer, leading the photocurrent to decrease, then output parameters of solar cell will decrease and if thickness decrease leads more photons which could be transmitted into the absorber layer to increasing photocurrent, this agreement with researchers [3].

The effect of increase doping concentration, we note that the slightly decrees when increasing the concentration on the output parameters solar cell within the range (1E18-1E19) cm⁻³. The increase in carrier recombination due to high doping concentrations could justify this. Large traps for charge carriers are created in highly doped buffer layers, increasing the probability of interaction, the trap concentration has an inverse relationship with the charge carrier lifetime, as a result, the recombination rate rises, contributing to a decrease in open circuit voltage and fill factor [12]. then the best thickness is (30)nm and best doping concentration is (1E18) cm⁻³ at same output parameters solar cell above. These results we obtained are better than the practical results [8].

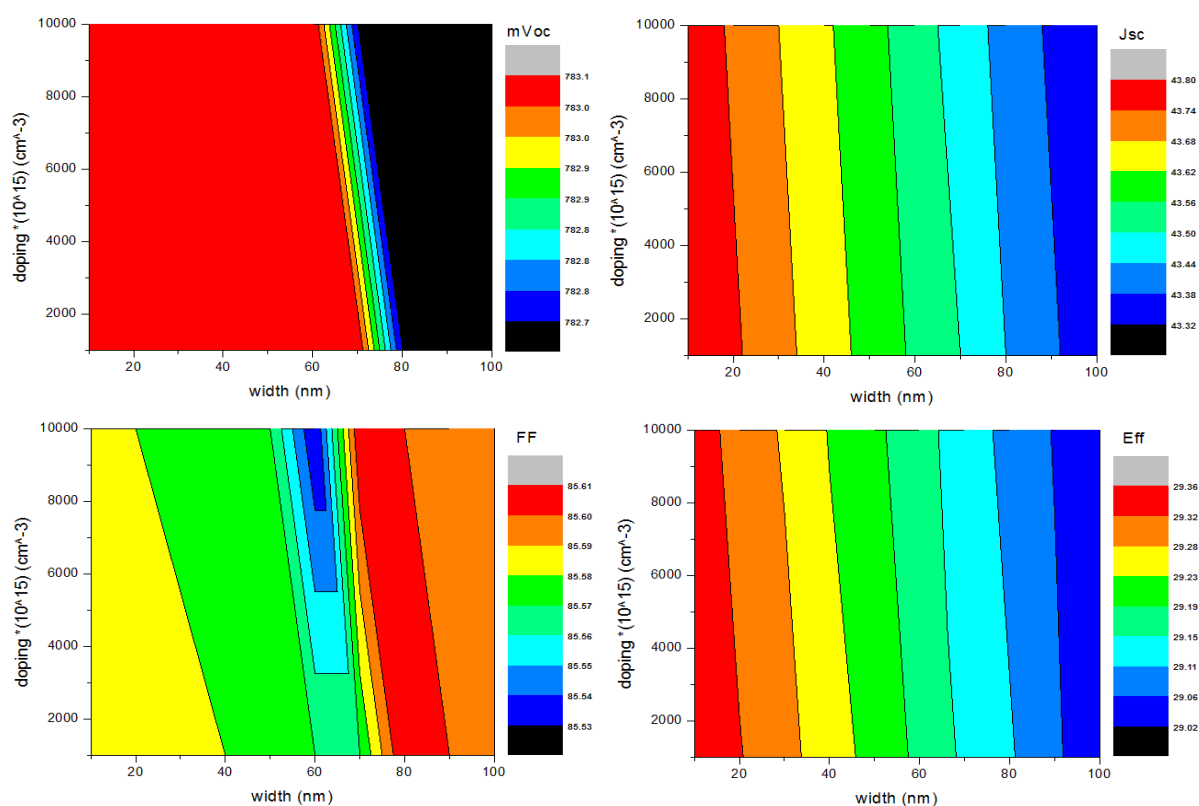


Fig. 2 Photovoltaic parameters as function of changing the thickness with changing the doping concentration of BZO buffer layer

c- Effect defect on cell:

Now we will study the effect of cell 1 consisting of absorption layer with thickness (1400)nm with concentration $(1E17)cm^{-3}$, and a buffer layer with thickness (30)nm with concentration $(1E18)cm^{-3}$, and thus we get the solar cell 1 (CIGSSe/BZO) without defects. From the voltage current diagram shown in Figure (3a) we obtain the output parameters of the solar cell V_{oc} , J_{sc} , FF, Eff equal (633.6mV, 39.97mA/cm², 80.25%, 20.32%) respectively.

Then we add the window layer (ZMO) with thickness (100)nm with concentration $(1E20)cm^{-3}$ without defects with the same variables for the absorption layer and the buffer layer of thickness and concentration, and thus the cell 2 is (CIGSSe/BZO/ZMO), from the voltage current diagram shown in Figure (3a), we obtain the output parameters of the solar cell V_{oc} , J_{sc} , FF, Eff equal (633.6mV, 40.05mA/cm², 80.3%, 20.37%) respectively, we note that properties of cell is improved by add (ZMO) layer.

Then we add the back surface field layer (BSF) with thickness (10)nm with concentration $(1E20)$, without defects with the same variables for the absorption layer, the buffer layer and the window layer of thickness and concentration, so that the cell 3 (MoS₂/CIGSSe/BZO/ZMO), from the voltage current diagram shown in Figure (3a) we obtain the output parameters of the solar cell V_{oc} , J_{sc} , FF, Eff equal (901.6mV, 43.71mA/cm², 87.19%, 34.36%) respectively,

We note that properties of cell is improved by add (MoS₂) layer, In this region the quality of the collector efficiency increases near the back electrode and for this reason the short circuit current increases, as for the improvement of the open circuit voltage, it results from the decrease in the saturation current with the presence of the back-surface field. The back pole can be used as a reflective material to give a second chance for the wavelengths to be absorbed and thus improve the performance of the solar cell at a low temperature during work.

Then we add the defects to cell 3 and notice that the output parameters of the solar cell are V_{oc} , J_{sc} , FF, Eff equal (783.1mV, 43.7 mA/cm², 85.59%, 29.29%) respectively, we note the defects have a strong effect on the performance of the solar cell because the defect reduces on open circuit voltage, short circuit current After that, the cell's performance will decrease.

Through the quantum efficiency diagram shown in Figure (3b), where the highest cell efficiency is (3,4,2,1) respectively, as the efficiency increases with the increase in the absorbance in the absorption layer, and thus the formation of the electron pair gap increases.

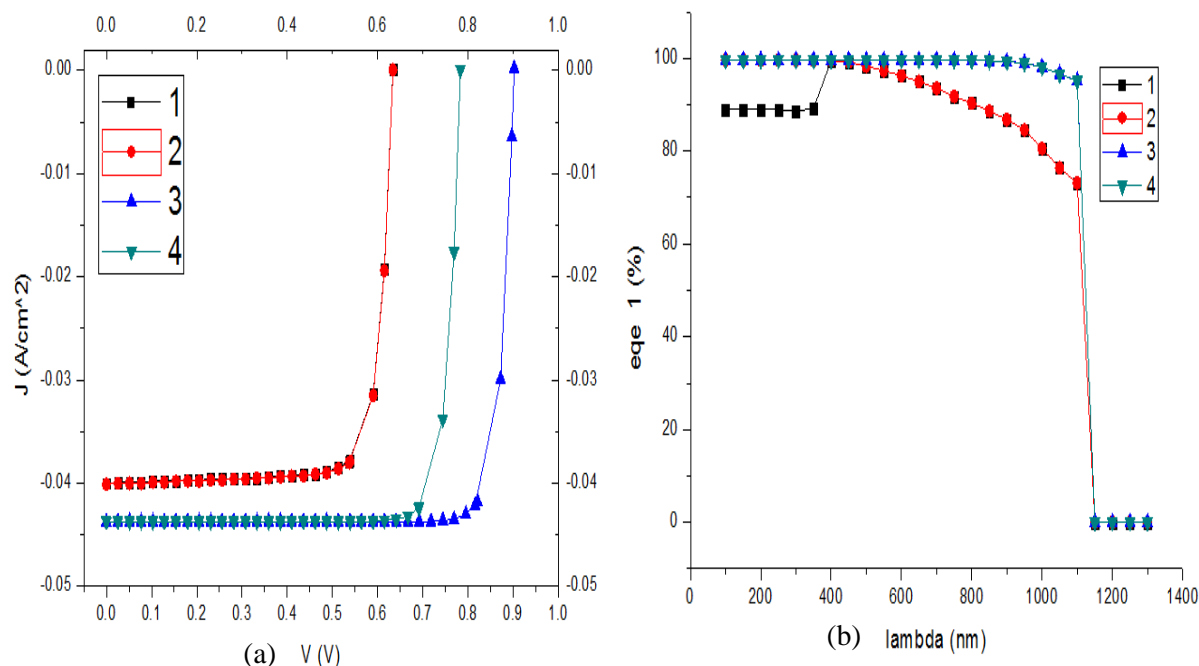


Fig.3 a: I-V diagram, b: quantum efficiency diagram for different cell.

Effect of change buffer layer:

now we change buffer layer in cell (MoS₂/CIGSSe/BZO/ZMO) at same parameter of thickness and concentration doping of MoS₂ (10nm) (1E20), absorber (1400nm) (1E17), buffer (30nm) (1E18), window (100nm) (1E20) layers, respectively. the parameters of different buffer layers it shown in table (4). The output parameters of these solar cells from I-V diagram it shown in figure (4a), we note that best efficiency at 29.29% for BZO layer, then 29.21%, 28.77%, 28.74%, 27.93%, for In₂S₃, CdS, ZnS, ZnSe, respectively. we can explain these different of quantum efficiency by figure (4b), because there is little difference in the quantum efficiency at short wavelengths and there is no difference at long wavelengths. The compare between of these results of open circuit voltage, short circuit current, fill factor, quantum efficiency it shown in table (5). from these results the (BZO) layer is a good buffer layer and ZnSe buffer layer is lest efficiency.

Table 4. different buffer layers

parameters	Symbol (unit)	BZO	ZnS [15]	CdS [16]	ZnSe [17]	In ₂ S ₃ [18]
Thickness	d (cm)	3E-6	3E-6	3E-6	3E-6	3E-6
Dielectric constant	dk	9	8.32	10	10	13.5
Electron Affinity	χ (eV)	4.55	4.5	4.2	4.2	4.45
Band gap	Eg (eV)	3.3	3.68	2.4	2.9	2.3
Density of states in CB	Nc (cm-3)	3E18	1.5E18	2.2E18	2E18	1.8E19

Density of states in VB	Nv(cm-3)	1.8E19	1.8E19	1.8E19	1.8E19	4E13
Electron mobility	μ_n (cm ² /Vs)	100	250	100	70	400
Hole mobility	μ_p (cm ² /Vs)	31	40	25	3	210
Acceptor concentration	Na (cm-3)	0	0	0	0	0
Donor concentration	Nd (cm-3)	1E20	1E18	1E18	1E18	1E18
Thermal velocity of electron and hole	v (cm/s)	1E07	1E07	1E07	1E07	1E07
density	Rho (g*cm-3)	5.61	4.09	4.82	5.27	4.9

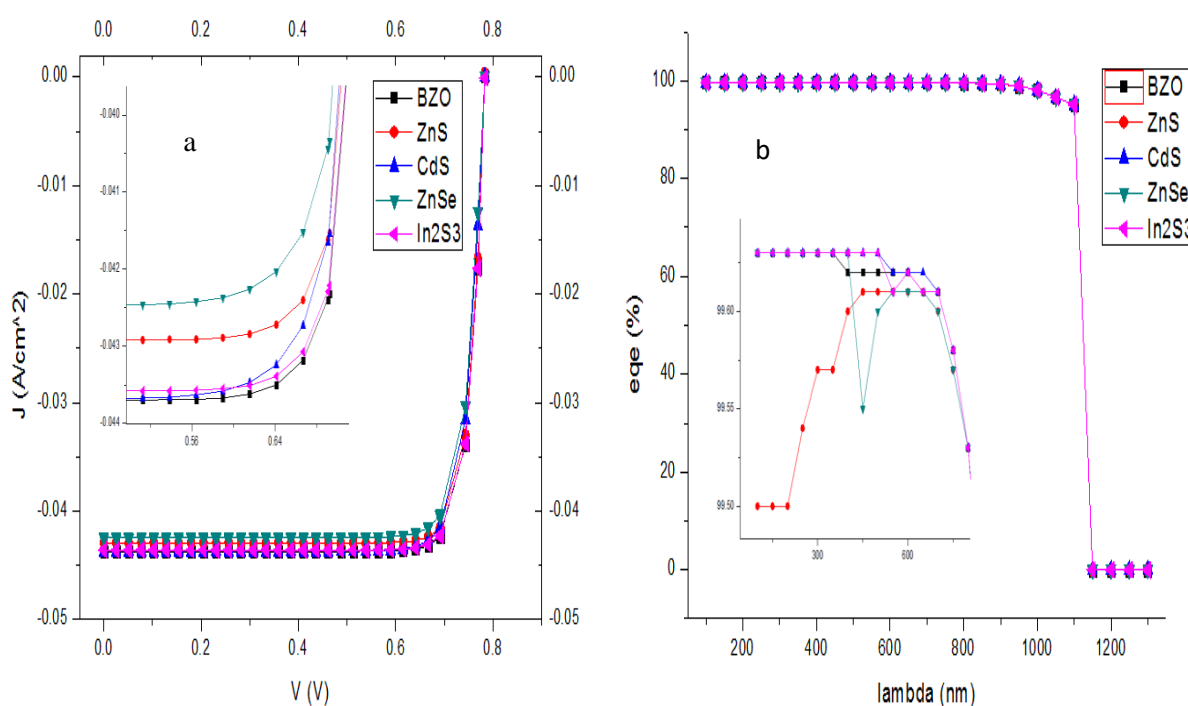


Fig. (4) a: I-V diagram b: quantum efficiency, for different buffer layer.

Table (5) compare between deferent buffer layer

buffers layers	Voc (mV)	Jsc (mA/cm ²)	FF (%)	Eff (%)
ZnO: B	783.1	43.7	85.59	29.29
ZnS	782.7	42.92	85.57	28.74
CdS	779.8	43.69	84.43	28.77
ZnSe	779	42.49	84.4	27.93
In2S3	783.1	43.58	85.6	29.21

Conclusion:

The cell performance has been analyzed and simulated by the variation of thickness layer with doping concentration for absorber and buffer layers using FORS-HET software as well as demonstrated the effect on the solar cell parameters like open circuit voltage (V_{oc}), short-circuit current density (J_{sc}), Fill Factor (FF), conversion efficiency ($\eta\%$). The optimum thickness and doping concentration of CIGSSe (1400nm, $1E17cm^{-3}$), BZO (30nm, $1E18cm^{-3}$), ZMO (100nm, $1E20cm^{-3}$) respectively. The optimum conversion efficiency is 29.29% has been observed. We can also take the effect of the types of Buffer on the properties of the solar cell and find the best types of buffer layer is (BZO) efficiently 29.9%, then 29.21%, 28.77%, 28.74%, 27.93%, for In₂S₃, CdS, ZnS, ZnSe, respectively. From these results we can use the BZO and In₂S₃ buffer layers as an alternative to the CdS layer.

References:

- [1] T. Feurer *et al.*, "Progress in thin film CIGS photovoltaics—Research and development, manufacturing, and applications," vol. 25, no. 7, pp. 645-667, 2017.
- [2] J. Park and M. J. E. Shin, "Numerical optimization of gradient bandgap structure for CIGS solar cell with ZnS buffer layer using technology computer-aided design simulation," vol. 11, no. 7, p. 1785, 2018.
- [3] M. Nakamura, K. Yamaguchi, Y. Kimoto, Y. Yasaki, T. Kato, and H. J. I. J. o. P. Sugimoto, "Cd-free Cu (In, Ga)(Se, S) 2 thin-film solar cell with record efficiency of 23.35%," vol. 9, no. 6, pp. 1863-1867, 2019.
- [4] M. Bär *et al.*, "Replacement of the CBD–CdS buffer and the sputtered i-ZnO layer by an ILGAR-ZnO WEL: optimization of the WEL deposition," vol. 75, no. 1-2, pp. 101-107, 2003.
- [5] A. Delahoy, J. Bruns, L. Chen, M. Akhtar, Z. Kiss, and M. Contreras, "Advances in large area CIGS technology," in *Conference Record of the Twenty-Eighth IEEE Photovoltaic Specialists Conference-2000 (Cat. No. 00CH37036)*, 2000, pp. 1437-1440: IEEE.
- [6] S. Chaisitsak, A. Yamada, and M. J. M. O. P. L. A. Konagai, "Comprehensive study of light-soaking effect in ZnO/Cu (InGa) Se₂ solar cells with Zn-based buffer layers," vol. 668, 2001.
- [7] V. Khomyak, I. Shtepliuk, V. Khranovskyy, and R. J. V. Yakimova, "Band-gap engineering of ZnO_{1-x}S_x films grown by rf magnetron sputtering of ZnS target," vol. 121, pp. 120-124, 2015.
- [8] S. Ishizuka, J. Nishinaga, T. Koida, and H. J. A. P. E. Shibata, "An over 18%-efficient completely buffer-free Cu (In, Ga) Se₂ solar cell," vol. 11, no. 7, p. 075502, 2018.
- [9] M. Bär *et al.*, "Determination of the band gap depth profile of the pentenary Cu (In (1- X) Ga X)(SY Se (1- Y)) 2 chalcopyrite from its composition gradient," vol. 96, no. 7, pp. 3857-3860, 2004.
- [10] A. Avellan *et al.*, "Simulation of Different Interface Configurations of CIGSSe Solar Cells," 2012.
- [11] H. Rashid, K. Rahman, M. Hossain, N. Tabet, F. Alharbi, and N. J. C. L. Amin, "Prospects of molybdenum disulfide (MoS₂) as an alternative absorber layer material in thin film solar cells from numerical modeling," vol. 11, no. 8, pp. 397-403, 2014.

- [12] X. He, Y. Song, L. Wu, C. Li, J. Zhang, and L. J. M. R. E. Feng, "Simulation of high-efficiency CdTe solar cells with Zn_{1-x}Mg_xO window layer by SCAPS software," vol. 5, no. 6, p. 065907, 2018.
- [13] S. Ouédraogo, F. Zougmore, and J. J. I. J. o. P. Ndjaka, "Numerical analysis of copper-indium-gallium-diselenide-based solar cells by SCAPS-1D," vol. 2013, 2013.
- [14] Y. Hirai, Y. Kurokawa, and A. J. J. J. o. A. P. Yamada, "Numerical study of Cu (In, Ga) Se₂ solar cell performance toward 23% conversion efficiency," vol. 53, no. 1, p. 012301, 2013.
- [15] S. Tobbeche, S. Kalache, M. Elbar, M. N. Kateb, M. R. J. O. Serdouk, and Q. Electronics, "Improvement of the CIGS solar cell performance: structure based on a ZnS buffer layer," vol. 51, no. 8, pp. 1-13, 2019.
- [16] M. S. R. Robin, M. M. M. Rasmi, M. S. Z. Sarker, and A. R. Al Mamun, "Numerical modeling and analysis of ultra thin film Cu (In, Ga) Se₂ solar cell using SCAPS-1D," in *2016 3rd International Conference on Electrical Engineering and Information Communication Technology (ICEEICT)*, 2016, pp. 1-5: IEEE.
- [17] J. Qu *et al.*, "Simulation of double buffer layer on CIGS solar cell with SCAPS software," vol. 51, no. 12, pp. 1-14, 2019.
- [18] N. Khoshsirat and N. A. M. J. J. o. E. M. Yunus, "Numerical Analysis of In₂S₃ Layer Thickness, Band Gap and Doping Density for Effective Performance of a CIGS Solar Cell Using SCAPS," vol. 45, no. 11, pp. 5721-5727, 2016.